

## Article

# Fast Terminal Sliding Control of Underactuated Robotic Systems Based on Disturbance Observer with Experimental Validation

Thaned Rojsiraphisal <sup>1</sup>, Saleh Mobayen <sup>2,\*</sup>, Jihad H. Asad <sup>3</sup>, Mai The Vu <sup>4,\*</sup>, Arthur Chang <sup>5</sup>  
and Jirapong Puangmalai <sup>6</sup>

- <sup>1</sup> Advanced Research Center for Computational Simulation, Department of Mathematics, Faculty of Science, Chiang Mai University, Chiang Mai 50200, Thailand; thaned@gmail.com
- <sup>2</sup> Future Technology Research Center, National Yunlin University of Science and Technology, 123 University Road, Section 3, Douliou, Yunlin 64002, Taiwan
- <sup>3</sup> Department of Physics, Faculty of Applied Sciences, Palestine Technical University, Tulkarm P.O. Box 7, Palestine; j.asad@ptuk.edu.ps
- <sup>4</sup> School of Intelligent Mechatronics Engineering, Sejong University, Seoul 05006, Korea
- <sup>5</sup> Bachelor Program in Interdisciplinary Studies, National Yunlin University of Science and Technology, Yunlin 64002, Taiwan; changart@yuntech.edu.tw
- <sup>6</sup> Department of Mathematics, Faculty of Education, Kamphaeng Phet Rajabhat University, Kamphaeng Phet 62000, Thailand; Puangmalai.J@gmail.com
- \* Correspondence: mobayens@yuntech.edu.tw (S.M.); maithevu90@sejong.ac.kr (M.T.V.)



**Citation:** Rojsiraphisal, T.; Mobayen, S.; Asad, J.H.; Vu, M.T.; Chang, A.; Puangmalai, J. Fast Terminal Sliding Control of Underactuated Robotic Systems Based on Disturbance Observer with Experimental Validation. *Mathematics* **2021**, *9*, 1935. <https://doi.org/10.3390/math9161935>

Academic Editor: Eva H. Dulf

Received: 27 May 2021

Accepted: 8 August 2021

Published: 13 August 2021

**Publisher's Note:** MDPI stays neutral with regard to jurisdictional claims in published maps and institutional affiliations.



**Copyright:** © 2021 by the authors. Licensee MDPI, Basel, Switzerland. This article is an open access article distributed under the terms and conditions of the Creative Commons Attribution (CC BY) license (<https://creativecommons.org/licenses/by/4.0/>).

**Abstract:** In this study, a novel fast terminal sliding mode control technique based on the disturbance observer is recommended for the stabilization of underactuated robotic systems. The finite time disturbance observer is employed to estimate the exterior disturbances of the system and develop the finite time control law. The proposed controller can regulate the state trajectories of the underactuated systems to the origin within a finite time in the existence of external disturbances. The stability analysis of the proposed control scheme is verified via the Lyapunov stabilization theory. The designed control law is enough to drive a switching surface achieving the fast terminal sliding mode against severe model nonlinearities with large parametric uncertainties and external disturbances. Illustrative simulation results and experimental validations on a cart-inverted pendulum system are provided to display the success and efficacy of the offered method.

**Keywords:** disturbance observer; fast terminal sliding mode; finite time convergence; Lyapunov stability; underactuated robotic system

## 1. Introduction

Underactuated systems are categories of nonlinear dynamic systems which have fewer number of actuators than degrees of freedom [1–5]. The stabilizer and tracker design problems of these dynamical structures involve wide investigation due to their application in flexible manipulators [6], marine vessels [7], robotics [8,9], aircraft assembly [10], hovercraft [11], legged locomotion [12], overhead crane [13], satellite [14], rigid spacecraft [15], inverted pendulum [16], aeroelastic wing section [17], underwater vehicles [18], surface vessels [19], quad-rotors [20,21], flexible joint robots [22], cranes [23], visual servoing [24], proprioceptive tactile sensing [25], vertical take-off and landing drones [26] etc. Due to low numbers of actuators, the used energy and complexity of underactuated systems are less than fully actuated systems. This class of systems, as stated in [16], cannot be stabilized (controlled) by smooth-feedback control laws since the dynamical structures of these systems are based on differential equations in the existence of nonintegrable differential circumstances [27]. Hence, the control of underactuated systems is a challenging issue. Furthermore, the control methods differ from case to case for underactuated systems and generally, may not be employed to the entire class [28].

In past years, much consideration has been paid for tracking control and stabilization of the underactuated structures. Numerous control methods, for instance, Lyapunov redesign [29], passivity-based control [30], optimal control [31], input-output linearization [32], backstepping control [33], nonlinear state-feedback control [34], anti-swing control [35], artificial neural network [36], fuzzy control [37], feedforward control [38],  $H_\infty$  control [39], coupling-based control [40], adaptive predictive control [41] and sliding mode control (SMC) [42] have been proposed to design proper trackers and stabilizers of underactuated dynamical systems. SMC is a well-known control technique for design of the robust stabilizers and trackers of various dynamical systems with uncertainty and external perturbation [43–45]. SMC offers a discontinuous controller to force the state trajectories to a switching surface and holds the state trajectories on a sliding surface afterwards [46]. The main features of SMC are reasonable robustness and suitable transient efficiency in the existence of perturbations. Additionally, the advantages of SMC comprise the robustness in contradiction of external disturbances and parametric variations, fast response, easiness of usage and satisfied stability. Generally, the design scheme of SMC covers two main stages [47,48]: (a) proposition of an appropriate switching surface; (b) presentation of a proper control input. The primary stage comprises the choice of a suitable sliding surface so that it forces the errors to remain along with the surface [49]. The next stage includes the design of an appropriate control signal which forces errors to reach the sliding surface. When the error states reach the switching surface, the system's order is decreased. Consequently, the control system dominates the exterior perturbations and matched parametric uncertainties [50]. In recent decades, SMC has been applied on several systems, for instance, flexible spacecraft [51], chaotic flow [52], electric vehicles [53], active suspension systems [54], electro-pneumatic actuators [55], aircraft [56], robot manipulators [57], missile guidance [58], unmanned aerial vehicles [59], nonholonomic robots [60], and other industrial systems. The traditional SMC approach has some significant weaknesses where the system's robust performance is not fulfilled in reaching mode and occurs high-frequency oscillations in the controller input. The linear SMC surfaces propose asymptotic stability in switching mode and hence, the state responses of the system are convergent to the origin with infinite time.

In comparison with common SMC procedure, a terminal sliding mode control (TSMC) scheme provides excellent characteristics, for instance, fast and finite time convergence [61]. For realizing the states' finite time convergence, the TSMC technique has been developed [62]. TSMC is mainly proper for high precision control, since it accelerates the rate of the convergence near equilibria. Actually, this procedure not only has the benefits of the sliding mode controller, however also enhances the stability and convergence speed near the origin [63]. The TSMC method has two problems: (a) it may suffer from singularity; (b) while the states are far away from the origin, this method has slower convergence than linear SMC. In past years, to realize the strong robustness and faster convergence, the fast TSMC (FTSMC) has been suggested. In the last decade, there has been more attention in the employment of this technique on several control problems [64]. Essentially, the fast convergence rate of states is achieved when the initial condition is far from origin [65]. Hence, the design of FTSMC has theoretical importance. Firstly, reference [66] introduced FTSMC approach for the stabilization of single-input single-output (SISO) dynamical systems. A global FTSMC technique is suggested in [67] for  $n$ -link robotic manipulators. In [68], a nonsingular FTSMC approach is applied to vehicular following systems. In [69], the nonsingular FTSMC method is proposed for the nonlinear dynamical systems. The adaptive control law is designed in [70] for a micro-electro-mechanical system gyroscope using global FTSMC and fuzzy neural network methods. In [71], an adaptive nonsingular FTSMC procedure involving robust control and adaptations laws is investigated for electro-mechanical actuators. The nonsingular integral FTSMC procedure is investigated in [72] for nonlinear dynamical systems. However, it should be noted that FTSMC is still required to be further considered on robust performances to tackle the perturbations.

In [73], a hierarchical TSMC scheme is offered for nonlinear underactuated structures which drive the error states to the equilibrium in the finite time. A discontinuous control input based on FTSMC technique is proposed in [74] for the underactuated surface vessels. In [75], the position control problem is proposed for the underactuated space robot, and a hierarchical TSMC procedure is recommended. The tracking problem based on finite time control for an underactuated autonomous surface vessel is studied in [76] using a nonsingular TSMC approach. In [77], the control problem of an unmanned quad-rotor helicopter using the robust TSMC technique is studied. In [78], a hierarchical development of FTSMC strategy is planned for a category of underactuated structures. The TSMC approach for navigation of an underactuated unmanned underwater vehicle is studied in [79]. In [80], a robust nonlinear control scheme based on integral-TSMC is proposed by using integral-TSMC, which can exponentially drive an underactuated unmanned under-sea vehicle onto a prespecified path in constant forward speed. In [81], a nonsingular FTSMC is recommended for underactuated spacecraft formation without radial/in-track thrust. In [82], a singularity-free TSMC approach based on radial basis function is suggested for underactuated mechanical systems. In [83], the diving control problem for underactuated unmanned undersea vehicles with parametric perturbations and wave disturbances using backstepping-based integral-FTSMC is studied. The objective of reference [84] is to design a TSMC-based controller for the tracking and lateral motion of underactuated underwater autonomous systems. In [85], according to the mixture of TSMC and high-order sliding mode techniques, a robust finite time controller scheme is proposed for control of joint configuration of three-link planar underactuated manipulators. In [86], the tracking controller scheme of nonlinear underactuated robotic systems using an adaptive fuzzy hierarchical TSMC technique is proposed. In [87], using an adaptive TSMC technique and finite time stabilization theory, the underactuated ships follow the desired path in the finite time in the existence of unknown perturbations. In [88], the tracking problem of underactuated unmanned underwater vehicles is studied and a TSMC-based robust nonlinear control technique is developed. A hierarchical FTSMC-based control design scheme is offered in [27] for a category of uncertain underactuated nonlinear structures. Compared to the former studies, no study is investigated about the FTSMC design based on the disturbance observer for stabilization of the underactuated systems with exterior disturbances. Actually, the environmental perturbations and parametric uncertainties are the principal difficulties for the stabilization of underactuated dynamical systems. The innovation of the present article is to design a new robust technique with fast and finite time convergence which improves the stabilization and robust performance of underactuated dynamical systems. Furthermore, the proposed disturbance observer satisfied the convergence of disturbance approximation errors to zero in the finite time. Finally, the suggested controller approach is used on a cart-inverted pendulum to approve the efficacy and proficiency of the process. The central novelties of the present research are listed as follows:

- (a) Design of a disturbance observer-based FTSMC technique for stabilization of underactuated systems with exterior perturbations.
- (b) Satisfaction of the stabilization of the state trajectories based on Barbalat's lemma.
- (c) Finite time convergence of disturbance approximation error to zero using the disturbance observer law.
- (d) Confirmation of the proposed method by using the illustrative simulations and experimental assessments on the practical cart-inverted pole.

The remainder of the current paper is prepared as follows: the problem definition of the cart-inverted pole is provided in Section 2. Main results including the stabilization analysis and the design process of suggested technique are given in Section 3. Demonstrative simulation outcomes and some experimental studies on the practical cart-inverted pole are displayed in Section 4. Lastly, conclusions are provided in Section 5.

## 2. Problem Definition

The nonlinear second-order system with exterior disturbance is considered as [89]

$$\begin{aligned}\dot{x}_1(t) &= x_2(t), \\ \dot{x}_2(t) &= f(x, t) + b(x, t)u(t) + d(t),\end{aligned}\quad (1)$$

where  $x_1(t)$  and  $x_2(t)$  are states,  $b(x, t)$  and  $f(x, t)$  denote the nonlinear time-varying functions,  $u(t)$  specifies the controller signal, and  $d(t)$  signifies exterior perturbation. Generally, the exact representation of these systems is not in the canonical form. Then, the dynamical equation of underactuated systems (cart-inverted pendulum) is presented as

$$\begin{aligned}\dot{x}_1(t) &= x_2(t), \\ \dot{x}_2(t) &= f_1(x, t) + b_1(x, t)u(t) + d_1(t), \\ \dot{x}_3(t) &= x_4(t), \\ \dot{x}_4(t) &= f_2(x, t) + b_2(x, t)u(t) + d_2(t),\end{aligned}\quad (2)$$

where  $x_i(t)$  specify the state variables,  $f_1(x, t)$ ,  $f_2(x, t)$ ,  $b_1(x, t)$  and  $b_2(x, t)$  represent the invertible known functions demonstrating system's dynamics, and  $d_1(t)$  and  $d_2(t)$  indicate exterior perturbations.

**Assumption 1.** The nonlinear functions  $f_i(x, t)$ ,  $i = 1, 2$  and  $b_i(x, t)$ , and external disturbances  $d_i(t)$  are assumed differentiable.

The finite time convergence means that the system states converge to the equilibrium or reference trajectory in the finite time. In order to illustrate this notion obviously, the subsequent definition and lemma are introduced:

**Definition 1.** Consider the dynamic system  $\dot{x} = f(x)$ , where  $x \in R^n$ . If there exists a constant  $T > 0$  such that the condition  $\lim_{t \rightarrow T} \|x\| = 0$  is satisfied and  $\|x(t)\| \equiv 0$  for  $t \geq T$ , then the dynamic system is finite time stable.

For the dynamic system  $\dot{x} = f(x)$ ,  $x \in R^n$ , the origin is finite time stable, if there exists a nonempty neighbourhood of the origin  $\{0\} \in D \subseteq R^n$ , where: (a) the origin is Lyapunov stable in  $D \setminus \{0\}$ , (b) a settling time function  $T : D \setminus \{0\} \rightarrow R^+$  can be calculated so that the unique solution of the dynamic system ( $\chi_{x_0}(t)$ ) satisfies  $\lim_{t \rightarrow T(x_0)} \|\chi_{x_0}(t)\| = 0$  for all  $t \in [t_0, T(x_0)]$  and  $x_0 = x(t_0) \in D \setminus \{0\}$ .

**Lemma 1.** Assume that a continuous positive-definite function  $V$  fulfils the differential inequality as [90]:

$$\dot{V} \leq -\alpha V - \beta V^\eta, \quad \forall t \geq t_0, \quad V(t_0) \geq 0, \quad (3)$$

where  $\alpha$  and  $\beta$  signify two positive constants, and  $\eta$  denotes a ratio of two odd positive integers ( $1 > \eta > 0$ ). Then, for any given time  $t_0$ , the function  $V$  converges to the origin at least in a finite time  $t_r = t_0 + \frac{1}{\alpha(1-\eta)} \ln\left(\frac{\alpha V^{1-\eta}(t_0) + \beta}{\beta}\right)$ .

**Proof.** From (3), one can obtain  $-\frac{dV}{\alpha V + \beta V^\eta} \geq dt$ , where integrating it from  $t_0$  to  $T$  yields:  $-\int_{V(t_0)}^0 \frac{dV}{\alpha V + \beta V^\eta} \geq \int_{t_0}^T dt$  or  $-\int_{V(t_0)}^0 \frac{V^{-\eta} dV}{\alpha V^{1-\eta} + \beta} \geq \int_{t_0}^T dt$ . By using the integration action, one achieves  $\frac{1}{\alpha(1-\eta)} \{\ln(\alpha V^{1-\eta} + \beta) - \ln(\beta)\} \geq T - t_0$  or  $T \leq t_0 + \frac{1}{\alpha(1-\eta)} \ln\left(\frac{\alpha V^{1-\eta}(t_0) + \beta}{\beta}\right)$ .  $\square$

### 3. Main Results

In order to study the stabilization of the perturbed nonlinear system, the dynamical system (2) is rewritten as follows:

$$\dot{h}(t) = A_1 h(t) + B_1 \{f_1(x, t) + b_1(x, t)u + d_1(x, t)\}, \quad (4)$$

$$\dot{\lambda}(t) = A_2 \lambda(t) + B_2 \{f_2(x, t) + b_2(x, t)u + d_2(x, t)\}, \quad (5)$$

where  $h(t) = [x_1 x_2]^T$ ,  $\lambda(t) = [x_3 x_4]^T$ ,  $A_1 = A_2 = \begin{bmatrix} 0 & 1 \\ 0 & 0 \end{bmatrix}$ ,  $B_1 = B_2 = [01]^T$ . According to the pole-placement method, the terms  $k'x$  and  $k''x$  with  $k' = [\bar{k}_1, \bar{k}_2]$  and  $k'' = [\bar{k}_3, \bar{k}_4]$  are supposed, where the values of  $k'$  and  $k''$  are chosen so that the deterministic equalities  $\lambda^2 + \bar{k}_2\lambda + \bar{k}_1 = 0$  and  $\lambda^2 + \bar{k}_4\lambda + \bar{k}_3 = 0$  are stable. As a result, the dynamic systems with exponential stability are found as

$$\ddot{h}(t) + \bar{k}_2 \dot{h}(t) + \bar{k}_1 h(t) = 0, \quad (6)$$

$$\ddot{\lambda}(t) + \bar{k}_4 \dot{\lambda}(t) + \bar{k}_3 \lambda(t) = 0, \quad (7)$$

where the above equations confirm that  $h(t)$  and  $\lambda(t)$  converge to the origin. Accordingly, the dynamic systems (4) and (5) are updated as

$$\dot{h}(t) = (A_1 - B_1 k') h(t) + B_1 \{k' h(t) + f_1(x, t) + b_1(x, t)u + d_1(x, t)\}, \quad (8)$$

$$\dot{\lambda}(t) = (A_2 - B_2 k'') \lambda(t) + B_2 \{k'' \lambda(t) + f_2(x, t) + b_2(x, t)u + d_2(x, t)\}. \quad (9)$$

The control signals can be provided as the following transformations:

$$u' = b_1(x, t)^{-1} \{v' - f_1(x, t)\}, \quad (10)$$

$$u'' = b_2(x, t)^{-1} \{v'' - f_2(x, t)\}, \quad (11)$$

where  $v'$  and  $v''$  denote the new control inputs. The controllers (10) and (11) consist of two parts: the first parts are  $-b_1(x, t)^{-1} f_1(x, t)$  and  $-b_2(x, t)^{-1} f_2(x, t)$  which are used to eliminate the nonlinearities of the system, and the other parts are  $b_1(x, t)^{-1} v'$  and  $b_2(x, t)^{-1} v''$  which are given to attenuate the effects of external disturbances. If the control signals (10) and (11) are substituted into (8) and (9), one obtains

$$\dot{h}(t) = (A_1 - B_1 k') h(t) + B_1 \{v' + H'\}, \quad (12)$$

$$\dot{\lambda}(t) = (A_2 - B_2 k'') \lambda(t) + B_2 \{v'' + H''\}, \quad (13)$$

where  $H' = k' h(t) + d_1(x, t)$  and  $H'' = k'' \lambda(t) + d_2(x, t)$ . The external disturbance terms  $d_1(x, t)$  and  $d_2(x, t)$  are two continuous functions, and therefore, the functions  $H'$  and  $H''$  are also continuous. As a result, the dynamical systems (12) and (13) are completely controllable and can be stabilized by various robust control techniques.

**Remark 1.** In the case that the terms  $b_1(x, t)$  and  $b_2(x, t)$  are not invertible, similar to [91], the pseudoinverse expressions are provided by  $b_1(x, t)^+ = (b_1^T b_1)^{-1} b_1^T$  and  $b_2(x, t)^+ = (b_2^T b_2)^{-1} b_2^T$ .

The sliding surfaces are defined by

$$s_1(t) = z_1(t) - x_2(t) \quad (14)$$

$$s_2(t) = z_2(t) - x_4(t) \quad (15)$$

with  $z_1(t)$  and  $z_2(t)$  which are indicated by

$$\dot{z}_1(t) = -k_1 s_1(t) - \beta_1 \operatorname{sgn}(s_1(t)) - \varepsilon_1 s_1(t)^{\frac{p_0}{q_0}} - |f_1(x, t)| \operatorname{sgn}(s_1(t)) + b_1(x, t)u(t), \quad (16)$$

$$\dot{z}_2(t) = -k_2 s_2(t) - \beta_2 \operatorname{sgn}(s_2(t)) - \varepsilon_2 s_2(t)^{\frac{p_0}{q_0}} - |f_2(x, t)| \operatorname{sgn}(s_2(t)) + b_2(x, t)u(t), \quad (17)$$

where  $p_0$  and  $q_0$  are two odd positive integers ( $p_0 < q_0$ ). The design coefficients  $k_1, k_2, \varepsilon_1, \varepsilon_2, \beta_1$  and  $\beta_2$  are positive constants satisfying  $\beta_1 \geq |d_1(x, t)|$  and  $\beta_2 \geq |d_2(x, t)|$ . The terminal sliding disturbance estimators  $\hat{d}_1(t), \hat{d}_2(t)$  are specified as

$$\hat{d}_1(t) = -k_1 s_1(t) - \beta_1 \operatorname{sgn}(s_1(t)) - \varepsilon_1 s_1(t)^{\frac{p_0}{q_0}} - |f_1(x, t)| \operatorname{sgn}(s_1(t)) - f_1(x, t). \quad (18)$$

$$\hat{d}_2(t) = -k_2 s_2(t) - \beta_2 \operatorname{sgn}(s_2(t)) - \varepsilon_2 s_2(t)^{\frac{p_0}{q_0}} - |f_2(x, t)| \operatorname{sgn}(s_2(t)) - f_2(x, t). \quad (19)$$

**Theorem 1.** *The underactuated system is considered as (2) and the switching surfaces are defined as (14) and (15). Using the TSMC disturbance observers (18) and (19), the error trajectories of disturbance approximation converge to the origin in the finite time.*

**Proof.** Differentiating (14) and (15) in regard to time, and employing (16) and (17), one has

$$\dot{s}_1(t) = -k_1 s_1(t) - \beta_1 \operatorname{sgn}(s_1(t)) - \varepsilon_1 s_1(t)^{\frac{p_0}{q_0}} - |f_1(x, t)| \operatorname{sgn}(s_1(t)) - f_1(x, t) - d_1(t), \quad (20)$$

$$\dot{s}_2(t) = -k_2 s_2(t) - \beta_2 \operatorname{sgn}(s_2(t)) - \varepsilon_2 s_2(t)^{\frac{p_0}{q_0}} - |f_2(x, t)| \operatorname{sgn}(s_2(t)) - f_2(x, t) - d_2(t), \quad (21)$$

The Lyapunov candidate functional is constructed by

$$V_1(t) = \frac{1}{2} (s_1(t)^2 + s_2(t)^2), \quad (22)$$

where time-derivative of (22) is obtained as

$$\begin{aligned} \dot{V}_1(t) &= s_1(t)\dot{s}_1(t) + s_2(t)\dot{s}_2(t) \\ &= -k_1 s_1^2 - \beta_1 |s_1| - \varepsilon_1 s_1^{\frac{(p_0+q_0)}{q_0}} - |f_1(x, t)| s_1 - d_1(t) s_1 - |s_1| |f_1(x, t)| \\ &\quad - k_2 s_2^2 - \beta_2 |s_2| - \varepsilon_2 s_2^{\frac{(p_0+q_0)}{q_0}} - |s_2| |f_2(x, t)| - f_2(x, t) s_2 - d_2(t) s_2 \\ &\leq -(k_1 s_1^2 + k_2 s_2^2) - \varepsilon_1 s_1^{\frac{(p_0+q_0)}{q_0}} - \varepsilon_2 s_2^{\frac{(p_0+q_0)}{q_0}} \\ &\quad - |f_1(x, t)| |s_1| + |f_1(x, t)| |s_1| \\ &\quad - |f_2(x, t)| |s_2| + |f_2(x, t)| |s_2| \\ &\quad - \beta_1 |s_1| + |d_1(t)| |s_1| - \beta_2 |s_2| + |d_2(t)| |s_2| \\ &\leq -(k_1 s_1^2 + k_2 s_2^2) - \varepsilon_1 s_1^{\frac{(p_0+q_0)}{q_0}} - \varepsilon_2 s_2^{\frac{(p_0+q_0)}{q_0}} \\ &\leq -2 \min\{k_1, k_2\} V(t) - 2^{\frac{(p_0+q_0)}{2q_0}} \min\{\varepsilon_1, \varepsilon_2\} V(t)^{\frac{(p_0+q_0)}{2q_0}}. \end{aligned} \quad (23)$$

According to (23), one can conclude that  $s_1(t)$  and  $s_2(t)$  are convergent to zero in finite time. The estimation error  $\tilde{d}_1(t) (= \hat{d}_1(t) - d_1(t))$  is obtained from (2), (16) and (18) as

$$\begin{aligned}\tilde{d}_1(t) &= -k_1 s_1(t) - \beta_1 \operatorname{sgn}(s_1(t)) - \varepsilon_1 s_1(t)^{\frac{p_0}{q_0}} \\ &\quad - |f_1(x, t)| \operatorname{sgn}(s_1(t)) - f_1(x, t) \\ &\quad - (\dot{x}_2(t) - b_1(x, t)u(t) - f_1(x, t)) \\ &= \dot{z}_1(t) - \dot{x}_2(t) = \dot{s}_1(t),\end{aligned}\quad (24)$$

and the estimation error  $\tilde{d}_2(t) (= \hat{d}_2(t) - d_2(t))$  is attained from (2), (17) and (19) as

$$\begin{aligned}\tilde{d}_2(t) &= -k_2 s_2(t) - \beta_2 \operatorname{sgn}(s_2(t)) - \varepsilon_2 s_2(t)^{\frac{p_0}{q_0}} \\ &\quad - |f_2(x, t)| \operatorname{sgn}(s_2(t)) - f_2(x, t) \\ &\quad - (\dot{x}_4(t) - b_2(x, t)u(t) - f_2(x, t)) \\ &= \dot{z}_2(t) - \dot{x}_4(t) = \dot{s}_2(t).\end{aligned}\quad (25)$$

The Equations (24) and (25) clarify that according to convergence of switching curves in finite time to the equilibrium (as shown in condition (23)), the estimation errors  $\tilde{d}_1(t)$  and  $\tilde{d}_2(t)$  are convergent to the origin in the finite time.  $\square$

To propose the finite time stabilizers, the FTSMC manifolds are presented as

$$\Sigma_1(t) = \lambda_1 s_1(t) + \mu_1 s_1(t)^{p_0/q_0} + \dot{s}_1(t), \quad (26)$$

$$\Sigma_2(t) = \lambda_2 s_2(t) + \mu_2 s_2(t)^{p_0/q_0} + \dot{s}_2(t), \quad (27)$$

where  $\lambda_1, \lambda_2, \mu_1$  and  $\mu_2$  are positive constants. In what follows, to assure convergence of FTSMC manifolds to origin in finite time, a new theorem is proved.

**Theorem 2.** Consider the underactuated plant (2), sliding surfaces (14) and (15), and FTSMC manifolds (26) and (27). Using the control law as

$$\begin{aligned}\dot{u}(t) &= \aleph^{-1} \left\{ \gamma_1 \Sigma_1(t)^2 + \gamma_2 \Sigma_2(t)^2 + \kappa_1 |\Sigma_1(t)|^{p_0/q_0+1} \right. \\ &\quad + \kappa_2 |\Sigma_2(t)|^{p_0/q_0+1} + \Sigma_1(t) \left( \ddot{z}_1(t) - \dot{f}_1(x, t) + \dot{s}_1(t) \right. \\ &\quad + \left( \lambda_1 + \mu_1 \eta s_1(t)^{p_0/q_0-1} \right) \dot{s}_1(t) - \dot{b}_1(x, t)u(t) - \dot{\hat{d}}_1(t) \Big) \\ &\quad + \Sigma_2(t) \left( \left( \lambda_2 + \mu_2 \eta s_2(t)^{p_0/q_0-1} \right) \dot{s}_2(t) + \ddot{z}_2(t) - \dot{f}_2(x, t) \right. \\ &\quad \left. \left. - \dot{\hat{d}}_2(t) - \dot{b}_2(x, t)u(t) + \dot{s}_2(t) \right) \right\}\end{aligned}\quad (28)$$

where  $\aleph = \Sigma_1(t)b_1(x, t) + \Sigma_2(t)b_2(x, t)$ ,  $\gamma_1, \gamma_2, \eta, \kappa$  are some arbitrary positive scalars, then, the FTSMC manifolds are converged to zero in finite time and stay on it.

**Proof.** The Lyapunov candidate function is defined by

$$V_2(t) = 0.5 \left( \Sigma_1(t)^2 + \Sigma_2(t)^2 \right). \quad (29)$$

From (26) and (27), time-derivatives of  $\Sigma_1(t)$  and  $\Sigma_2(t)$  are achieved as

$$\begin{aligned}\dot{\Sigma}_1(t) &= \ddot{z}_1(t) - \ddot{x}_2(t) + \left( \lambda_1 + \mu_1 \eta s_1(t)^{p_0/q_0-1} \right) \dot{s}_1(t) \\ &= -\dot{f}_1(x, t) + \ddot{z}_1(t) + \left( \lambda_1 + \mu_1 \eta s_1(t)^{p_0/q_0-1} \right) \dot{s}_1(t) \\ &\quad - \dot{d}_1(t) - \dot{b}_1(x, t)u(t) - b_1(x, t)\dot{u}(t)\end{aligned}\quad (30)$$

$$\begin{aligned}\dot{\Sigma}_2(t) &= \ddot{z}_2(t) - \ddot{x}_4(t) + \left(\lambda_2 + \mu_2 \eta s_2(t)^{p_0/q_0-1}\right) \dot{s}_2(t) \\ &= \ddot{z}_2(t) - \dot{d}_2(t) + \left(\lambda_2 + \mu_2 \eta s_2(t)^{p_0/q_0-1}\right) \dot{s}_2(t) \\ &\quad - \dot{f}_2(x, t) - b_2(x, t) \dot{u}(t) - \dot{b}_2(x, t) u(t)\end{aligned}\quad (31)$$

Differentiating  $V(t)$ , and by employing (30) and (31), we have

$$\begin{aligned}\dot{V}_2(t) &= \Sigma_1(t) \left\{ \ddot{z}_1(t) + \left(\lambda_1 + \mu_1 \eta s_1(t)^{p_0/q_0-1}\right) \dot{s}_1(t) \right. \\ &\quad \left. - \dot{b}_1(x, t) u(t) - \dot{f}_1(x, t) - b_1(x, t) \dot{u}(t) - \dot{d}_1(t) \right\} \\ &\quad + \Sigma_2(t) \left\{ \ddot{z}_2(t) + \left(\lambda_2 + \mu_2 \eta s_2(t)^{p_0/q_0-1}\right) \dot{s}_2(t) \right. \\ &\quad \left. - \dot{b}_2(x, t) u(t) - \dot{f}_2(x, t) - b_2(x, t) \dot{u}(t) - \dot{d}_2(t) \right\}.\end{aligned}\quad (32)$$

Replacing (28) into (32), we have

$$\begin{aligned}\dot{V}_2(t) &= \Sigma_1(t) \left\{ -\dot{d}_1(t) + \dot{\hat{d}}_1(t) - \ddot{s}_1(t) \right\} \\ &\quad + \Sigma_2(t) \left\{ -\dot{d}_2(t) + \dot{\hat{d}}_2(t) - \ddot{s}_2(t) \right\} \\ &\quad - \left\{ \kappa_1 |\Sigma_1(t)|^{p_0/q_0+1} + \kappa_2 |\Sigma_2(t)|^{p_0/q_0+1} \right. \\ &\quad \left. + \gamma_1 \Sigma_1(t)^2 + \gamma_2 \Sigma_2(t)^2 \right\}.\end{aligned}\quad (33)$$

Based on the results (24) and (25), two first terms of (33) are equal to zero and the subsequent inequality holds:

$$\begin{aligned}\dot{V}_2(t) &\leq -2 \min\{\gamma_1, \gamma_2\} V(t) \\ &\quad - 2^{\frac{(p_0/q_0+1)}{2}} \min\{\kappa_1, \kappa_2\} V(t)^{\frac{(p_0/q_0+1)}{2}}.\end{aligned}\quad (34)$$

Therefore, the Lyapunov function (29) approaches gradually to zero and the FTSMC manifolds (26) and (27) converge to the equilibrium in the finite time.  $\square$

**Remark 2.** It is obtained from (34) that derivative of the Lyapunov functional with respect to time is negative semi-definite and proves that Lyapunov function  $V(t)$  and FTSMC manifolds  $\Sigma_1(t)$  and  $\Sigma_2(t)$  are both bounded. It is concluded from (26) and (27) that  $s_1(t)$ ,  $s_2(t)$ ,  $\dot{s}_1(t)$  and  $\dot{s}_2(t)$  are all bounded functions. Because  $V(0)$  is a bounded scalar function and Lyapunov function is nonincreasing, one achieves that  $\lim_{t \rightarrow \infty} \int_0^t \|V(\tau)\| d\tau$ ,  $\lim_{t \rightarrow \infty} \int_0^t \|s_1(\tau)\| d\tau$  and  $\lim_{t \rightarrow \infty} \int_0^t \|s_2(\tau)\| d\tau$  are also bounded. Thus, due to Barbalat's lemma and the boundedness of the terms  $\lim_{t \rightarrow \infty} \int_0^t \|s_1(\tau)\| d\tau$ ,  $\lim_{t \rightarrow \infty} \int_0^t \|s_2(\tau)\| d\tau$ ,  $\dot{s}_1(t)$  and  $\dot{s}_2(t)$ , the sliding surfaces  $s_1(t)$  and  $s_2(t)$  converge to the origin, i.e.,  $\lim_{t \rightarrow \infty} \int_0^t s_1(\tau) d\tau = \lim_{t \rightarrow \infty} \int_0^t s_2(\tau) d\tau = 0$ .

Considering the fast terminal sliding mode controller expressed in (28), the terms  $s_1(t)^{p_0/q_0-1}$  and  $s_2(t)^{p_0/q_0-1}$  cause the singularity problem if  $s_1(t) = 0$  and  $s_2(t) = 0$  because of the negative power of the sliding surfaces. Hence, FTSMC cannot fulfill the bounded control action when  $s_1(t) = 0$  and  $s_2(t) = 0$ . Therefore, a nonsingular fast terminal sliding controller is offered to dominate the singularity problem.

The nonsingular FTSMC manifolds is proposed as

$$\Sigma_1(t) = \mu_1^{-1} (\dot{s}_1(t) + \lambda_1 s_1(t))^{q_0/p_0} + s_1(t), \quad (35)$$

$$\Sigma_2(t) = \mu_2^{-1} (\dot{s}_2(t) + \lambda_2 s_2(t))^{q_0/p_0} + s_2(t). \quad (36)$$

For elimination of the singularity problem of FTSMC and satisfaction of convergence of state variables to zero in finite time, the succeeding theorem is presented.



**Theorem 3.** Consider the disturbed underactuated system (2) and nonsingular fast terminal sliding surfaces (35) and (36). If the control input is employed as

$$\begin{aligned} \dot{u} = & \Xi^{-1} \left\{ \gamma_1 \Sigma_1(t)^2 + \gamma_2 \Sigma_2(t)^2 + \kappa_1 |\Sigma_1(t)|^{p_0/q_0+1} \right. \\ & + \kappa_2 |\Sigma_2(t)|^{p_0/q_0+1} + \Sigma_1(t) \left( \dot{s}_1 + \frac{q_0}{\mu_1 p_0} (\dot{s}_1 + \lambda_1 s_1)^{q_0/p_0-1} \right. \\ & \times (\ddot{z}_1(t) - \dot{b}_1(x, t)u(t) + \lambda_1 \dot{s}_1 - \dot{d}_1(t) + \ddot{s}_1 - \dot{f}_1(x, t)) \\ & + \Sigma_2(t) \left( \dot{s}_2 + \frac{q_0}{\mu_2 p_0} (\dot{s}_2 + \lambda_2 s_2)^{q_0/p_0-1} (\ddot{z}_2(t) - \dot{f}_2(x, t) \right. \\ & \left. \left. - \dot{b}_2(x, t)u(t) + \ddot{s}_2 - \dot{d}_2(t) + \lambda_2 \dot{s}_2) \right) \right\} \end{aligned} \quad (37)$$

with  $\Xi = \frac{q_0}{\mu_1 p_0} b_1(x, t) \Sigma_1(t) (\dot{s}_1 + \lambda_1 s_1)^{q_0/p_0-1} + \frac{q_0}{\mu_2 p_0} b_2(x, t) \Sigma_2(t) (\dot{s}_2 + \lambda_2 s_2)^{q_0/p_0-1}$ , then, the nonsingular FTSMC manifolds converge to origin in the finite time.

**Proof.** Construct the Lyapunov functional as (29). Differentiating  $\Sigma_1(t)$  and  $\Sigma_2(t)$ , and using (35) and (36), one finds

$$\dot{\Sigma}_1(t) = \dot{s}_1(t) + \frac{q_0}{\mu_1 p_0} (\ddot{s}_1(t) + \lambda_1 \dot{s}_1(t)) (\dot{s}_1(t) + \lambda_1 s_1(t))^{q_0/p_0-1} \quad (38)$$

$$\dot{\Sigma}_2(t) = \dot{s}_2(t) + \frac{q_0}{\mu_2 p_0} (\ddot{s}_2(t) + \lambda_2 \dot{s}_2(t)) (\dot{s}_2(t) + \lambda_2 s_2(t))^{q_0/p_0-1} \quad (39)$$

Differentiating Lyapunov functional (29) and using the second derivatives of (14) and (15), one attains

$$\begin{aligned} \dot{V}_2(t) = & \Sigma_1(t) \left\{ \dot{s}_1 + \frac{q_0}{\mu_1 p_0} (-\dot{f}_1(x, t) + \ddot{z}_1 - \dot{b}_1(x, t)u(t) \right. \\ & \left. - b_1(x, t)\dot{u}(t) - \dot{d}_1(t) + \lambda_1 \dot{s}_1) (\dot{s}_1 + \lambda_1 s_1)^{q_0/p_0-1} \right\} c \\ & + \Sigma_2(t) \left\{ \dot{s}_2 + \frac{q_0}{\mu_2 p_0} (\ddot{z}_2 - \dot{f}_2(x, t) - \dot{b}_2(x, t)u(t) \right. \\ & \left. - b_2(x, t)\dot{u}(t) - \dot{d}_2(t) + \lambda_2 \dot{s}_2) (\dot{s}_2 + \lambda_2 s_2)^{q_0/p_0-1} \right\}. \end{aligned} \quad (40)$$

Substituting (37) into (40) yields

$$\begin{aligned} \dot{V}_2(t) = & -\kappa_1 |\Sigma_1(t)|^{p_0/q_0+1} - \kappa_2 |\Sigma_2(t)|^{p_0/q_0+1} \\ & - \gamma_1 \Sigma_1(t)^2 - \gamma_2 \Sigma_2(t)^2 \\ & \leq -2 \min\{\gamma_1, \gamma_2\} V(t) \\ & - 2^{\frac{(p_0/q_0+1)}{2}} \min\{\kappa_1, \kappa_2\} V(t)^{\frac{(p_0/q_0+1)}{2}}. \end{aligned} \quad (41)$$

This result confirms that the nonsingular fast terminal sliding surface reaches the origin in the finite time and the state variables are convergent to origin.  $\square$

The block diagram of the proposed control technique is displayed in Figure 1, which demonstrates both disturbance estimator and finite time stabilizer parts.

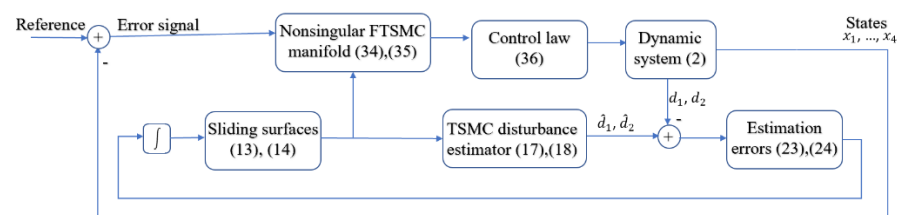


**Figure 1.** Block diagram of the proposed control method.

#### 4. Simulation and Experimental Outcomes

In order to validate the theoretical outcomes of proposed structure, a cart-inverted pendulum is considered in this section. In the studied system, the pendulum (pole) is stabilized in an upright situation. The fourth-order cart-inverted pendulum plant is in the form of an underactuated system [92]. The considered system is famous as a suitable balancing testbed to prove the efficiency of several control techniques. The principal issue in the stabilization of the considered pole is the nonlinear coupling goal in rotational/translational motions in the presence of sinusoidal functions. The dynamics of the cart-inverted pole exposed in Figure 2 is defined by the differential Equation (2), with [89]

$$f_1(x, t) = \frac{m_t g \sin(x_1) - 0.5 m_p L \sin(2x_1) x_2^2}{L \left( (4/3) m_t - m_p \cos(x_1)^2 \right)}, \quad (42)$$

$$f_2(x, t) = \frac{-(4/3) m_p L x_2^2 \sin(x_1) + 0.5 m_p g \sin(2x_1)}{(4/3) m_t - m_p \cos(x_1)^2} \quad (43)$$

$$b_1(x, t) = \frac{\cos(x_1)}{L \left( (4/3) m_t - m_p \cos(x_1)^2 \right)}, \quad (44)$$

$$b_2(x, t) = \frac{4}{3 \left( (4/3) m_t - m_p \cos(x_1)^2 \right)}, \quad (45)$$

where  $x_1(t)$  indicates pendulum angular position from vertical axis,  $x_2(t)$  denotes pendulum angular velocity from vertical axis,  $x_3(t)$  signifies cart position,  $x_4(t)$  shows cart velocity,  $g$  implies the gravity constant,  $L$  represents the half-length of the pendulum, and  $m_t$  signifies the system's mass (comprising pendulum's mass ( $m_p$ ) and cart's mass ( $m_c$ )). The initial states are given as  $[x_1(0), x_2(0), x_3(0), x_4(0)] = [(\pi/6), 0, -0.5, 0]$ . For simulation use, the coefficients of cart-pole system are specified as  $m_c = 1$  Kg,  $m_p = 0.3$  Kg,  $L = 0.25$  m and  $g = 9.8$  m/s<sup>2</sup>.

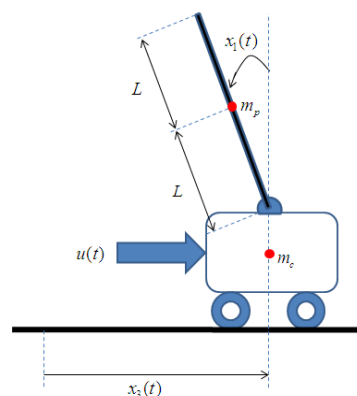
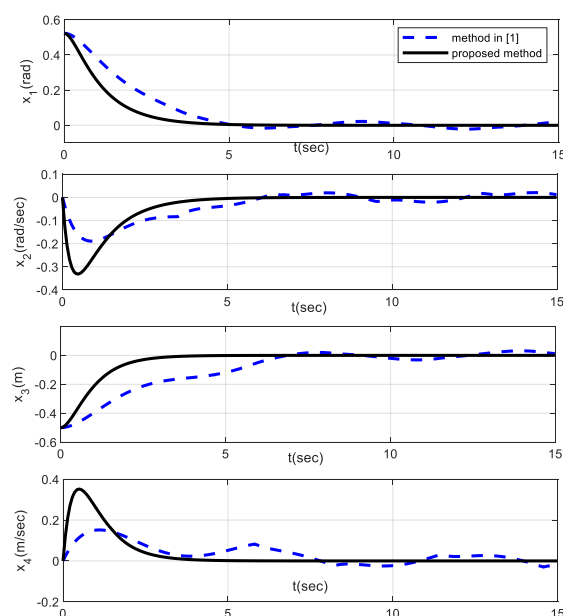


Figure 2. Schematic representation of cart-inverted pole.

The constants of sliding surfaces and control law are considered by trial and error as  $k_1 = 2$ ,  $k_2 = 1$ ,  $\varepsilon_1 = 0.7$ ,  $\varepsilon_2 = 0.5$ ,  $\lambda_1 = 2.5$ ,  $\lambda_2 = 3$ ,  $\kappa_1 = 2$ ,  $\kappa_2 = 1$ ,  $\beta_1 = 0.35$ ,  $\beta_2 = 0.25$  and  $\eta = 0.8$ . The exterior perturbations are taken as  $d_1(t) = 0.3 \sin(3t)$ ,  $d_2(t) = 0.2 \cos(1.5t)$ . It is displayed from the results that the proposed control technique effectively stabilizes the cart-inverted pole. Figure 3 displays the time history of the pendulum angular position which exhibits that the pendulum is stabilized from the initial state  $\pi/6$  in presence of nonlinearities and exterior disturbances. Moreover, the position of the cart is displayed in Figure 3. It is attained from this figure that the suggested approach keeps the cart in a short distance. Time trajectories of surfaces and FTSMC manifolds are plotted in Figures 4 and 5, which reveal that switching surfaces and FTSMC manifolds converge to the origin quickly.

Furthermore, as can be seen in Figure 5, there is a slight chattering problem in FTSMC manifolds according to the effects of perturbation and sign function. Figure 6 demonstrates the trajectory of the control input, which illustrates that the controller input found after integrating is a continuous signal and does not have any chattering. According to these results, it is obvious that the recommended controller procedure has satisfactory robust presentation in the existence of nonlinearities and perturbations.



**Figure 3.** Time history of pendulum angular position.

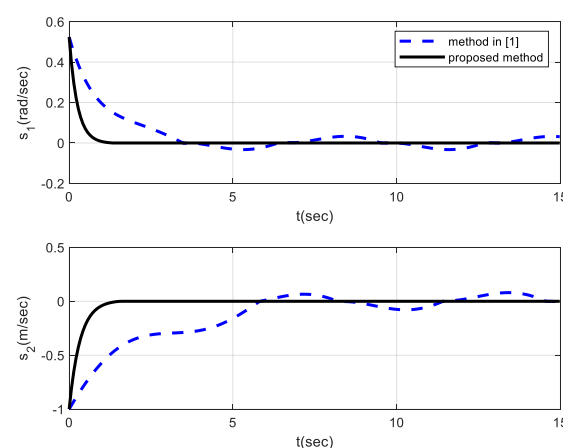


**Figure 4.** Time histories of switching curves.

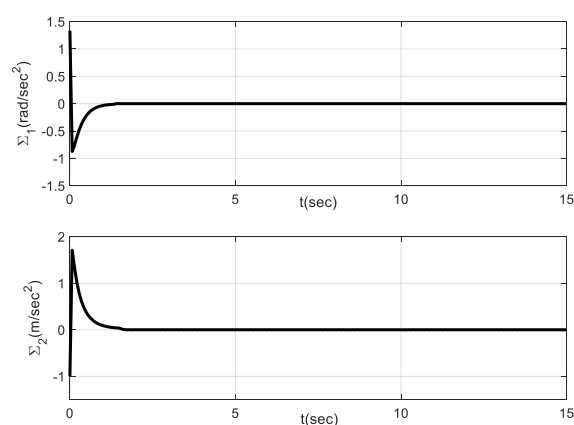


**Figure 5.** Time responses of FTSMC manifolds.

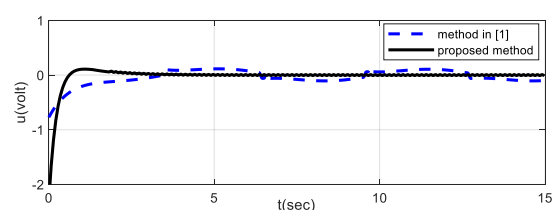


**Figure 6.** Time response of the control input.

**Remark 3.** A fair comparison is by making sure that the gains of the controllers are optimized and designed to ensure the best performance possible in each case. Once the optimum tracking performance is obtained, the comparison between the two approaches is performed. Additionally, both qualitative and quantitative parameters have been considered in the comparison analysis to ensure a fair comparison. In this paper, a fair comparison (quantitative and qualitative) has been performed and we have tried to consider the same qualitative and quantitative conditions in the simulation results by our proposed technique and the method in [1]. Though the sliding surfaces and control input laws of the proposed technique are simple, the simulation results of our control approach have less oscillations and all trajectories converge to the origin quickly.

Furthermore, the experimental operation of the proposed controller is provided by using MATLAB Real-Time and Simulink toolboxes (Figure 7). The angular situation of the pendulum and cart's position are both measured via Autonics® E40S encoders. The employed (input–output) card is PCI-1751 and builds the connection among the practical system and computer, and has digital to analog and analog to digital converters. Experimental outcomes for the angular position of the pole and the position of the cart are displayed in Figures 8 and 9. The angular position of the pole varies from  $-\pi^{rad}$  to zero, and then rests around the origin. These experimental assessments are reliable with the simulation outcomes which prove the performance of the suggested method. The cart's controller input is demonstrated in Figure 10. It is displayed in Figure 10 that no chattering occurs in the controller signal. In experimental outcomes, the time interval of swing-up obtains a high-amplitude action. This assessment on the real cart-inverted pendulum confirms that the proposed controller is practically efficient.

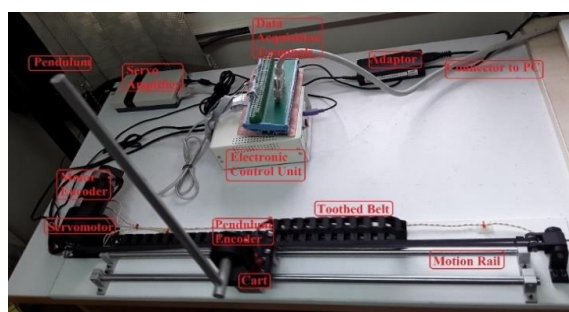


Figure 7. Experimental setup of inverted pendulum system.

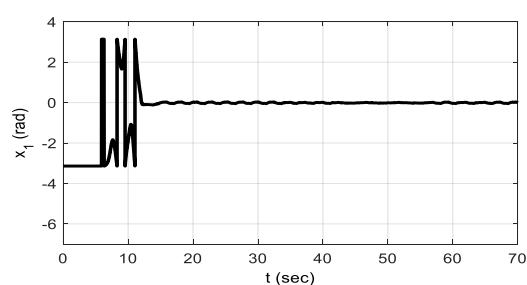


Figure 8. Time history of angular position of practical pendulum.

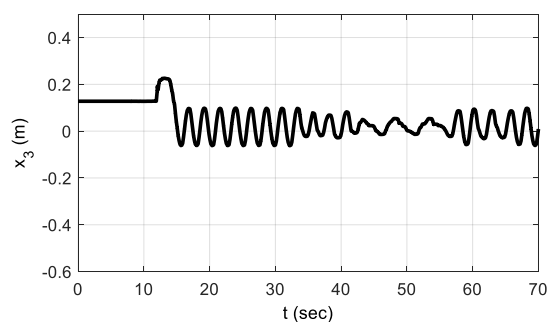


Figure 9. Time history of position of cart (experimental result).

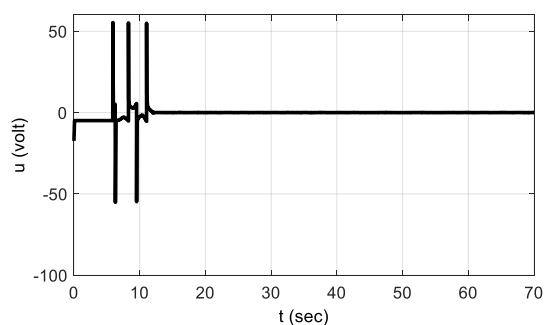


Figure 10. Control input of constructed system.

## 5. Conclusions

This study offers a fast terminal sliding mode control procedure according to the disturbance observer for the stabilization of underactuated systems with external perturbations. A robust controller procedure is developed with the result that the switching manifolds are convergent to equilibrium in the finite time. The proposed disturbance observer fulfills that the estimation error converges to equilibrium in the finite time. Moreover, the recommended controller methodology assures the stabilization of states. Numerical simulation results and practical validations on a cart-inverted pole verify the proficiency

and reliability of the planned technique. One of the important traits of this experimental application is employment of xPC-Target<sup>®</sup> toolbox and data acquisition (DAQ) card in Simulink<sup>®</sup> providing hardware-in-the-loop and rapid-prototype implementation. In the future research, we will work on adaptive event-trigger-based finite time robust tracking control of underactuated mechanical systems.

**Author Contributions:** Conceptualization, investigation, and writing—original draft preparation, T.R., S.M. and A.C.; writing—review and editing and supervision, J.H.A., M.T.V. and J.P. All authors have read and agreed to the published version of the manuscript.

**Funding:** This research received no external funding.

**Data Availability Statement:** The data that support the findings of this study are available within the article.

**Acknowledgments:** This research was partially supported by Chiang Mai University.

**Conflicts of Interest:** The authors declare no conflict of interest.

## References

- Pan, H.; Zhang, G.; Ouyang, H.; Mei, L. Novel fixed-time nonsingular fast terminal sliding mode control for second-order uncertain systems based on adaptive disturbance observer. *IEEE Access* **2020**, *8*, 126615–126627. [\[CrossRef\]](#)
- Kim, J.H.; Yoo, S.J. Nonlinear-Observer-Based Design Approach for Adaptive Event-Driven Tracking of Uncertain Underactuated Underwater Vehicles. *Mathematics* **2021**, *9*, 1144. [\[CrossRef\]](#)
- Rehman, F.U.; Mehmood, N.; Din, S.U.; Mufti, M.R.; Afzal, H. Adaptive Sliding Mode Based Stabilization Control for the Class of Underactuated Mechanical Systems. *IEEE Access* **2021**, *9*, 26607–26615. [\[CrossRef\]](#)
- Viswanathan, S.P.; Sanyal, A.K.; Samiei, E. Integrated Guidance and Feedback Control of Underactuated Robotics System in SE (3). *J. Intell. Robot. Syst.* **2018**, *89*, 251–263. [\[CrossRef\]](#)
- Idá, E.; Briot, S.; Carricato, M. Natural Oscillations of Underactuated Cable-Driven Parallel Robots. *IEEE Access* **2021**, *9*, 71660–71672. [\[CrossRef\]](#)
- Xin, X.; Liu, Y. A set-point control for a two-link underactuated robot with a flexible elbow joint. *J. Dyn. Syst. Meas. Control* **2013**, *135*, 051016. [\[CrossRef\]](#)
- Weng, Y.; Wang, N.; Soares, C.G. Data-driven sideslip observer-based adaptive sliding-mode path-following control of underactuated marine vessels. *Ocean. Eng.* **2020**, *197*, 106910. [\[CrossRef\]](#)
- Hamed, K.A.; Buss, B.G.; Grizzle, J.W. Continuous-time controllers for stabilizing periodic orbits of hybrid systems: Application to an underactuated 3D bipedal robot. In Proceedings of the IEEE 53rd Annual Conference on Decision and Control (CDC), Los Angeles, CA, USA, 15–17 December 2014; pp. 1507–1513.
- Disyadej, T.; Kwanmuang, S.; Muneesawang, P.; Promjan, J.; Pochinapan, K. Smart Transmission Line Maintenance and Inspection using Mobile Robots. *Adv. Sci. Technol. Eng. Syst. J.* **2020**, *5*, 493–500. [\[CrossRef\]](#)
- Roy, B.; Asada, H. Nonlinear Feedback Control of a Gravity-Assisted Underactuated Manipulator With Application to Aircraft Assembly. *IEEE Trans. Robot.* **2009**, *25*, 1125–1133. [\[CrossRef\]](#)
- Muñoz-Mansilla, R.; Chaos, D.; Díaz, J.; Aranda, J. Application of quantitative feedback theory techniques for the control of a non-holonomic underactuated hovercraft. *IET Control Theory Appl.* **2012**, *6*, 2188–2197. [\[CrossRef\]](#)
- Berkemeier, M.D.; Fearing, R.S. Control experiments on an underactuated robot with application to legged locomotion. In Proceedings of the IEEE International Conference on Robotics and Automation, San Diego, CA, USA, 8–13 May 1994; pp. 149–154.
- Lu, B.; Fang, Y.; Sun, N. Sliding mode control for underactuated overhead cranes suffering from both matched and unmatched disturbances. *Mechatronics* **2017**, *47*, 116–125. [\[CrossRef\]](#)
- Alamir, M.; Boyer, F. Fast Generation of Attractive Trajectories for an Under-Actuated Satellite Application to Feedback Control Design. *Optim. Eng.* **2003**, *4*, 215–230. [\[CrossRef\]](#)
- Zeng, W.; Wang, Q. Learning from adaptive neural network control of an underactuated rigid spacecraft. *Neurocomputing* **2015**, *168*, 690–697. [\[CrossRef\]](#)
- Riachy, S.; Orlov, Y.; Floquet, T.; Santiesteban, R.; Richard, J.P. Second-order sliding mode control of underactuated mechanical systems I: Local stabilization with application to an inverted pendulum. *Int. J. Robust Nonlinear Control* **2008**, *18*, 529–543. [\[CrossRef\]](#)
- Wei, X.; Mottershead, J.E. Robust passivity-based continuous sliding-mode control for under-actuated nonlinear wing sections. *Aerosp. Sci. Technol.* **2017**, *60*, 9–19. [\[CrossRef\]](#)
- Bi, F.; Wei, Y.; Zhang, J.; Cao, W. Position-tracking control of underactuated autonomous underwater vehicles in the presence of unknown ocean currents. *IET Control Theory Appl.* **2010**, *4*, 2369–2380. [\[CrossRef\]](#)
- Yoo, S.J.; Park, B.S. Guaranteed performance design for distributed bounded containment control of networked uncertain underactuated surface vessels. *J. Frankl. Inst.* **2017**, *354*, 1584–1602. [\[CrossRef\]](#)

20. Yih, C.-C. Robust Flight Control of an Underactuated Quadrotor via Sliding Modes. In *Applications of Sliding Mode Control*; Springer: Singapore, 2017; pp. 87–104.
21. Zhang, Y.; Chen, Z.; Zhang, X.; Sun, Q.; Sun, M. A novel control scheme for quadrotor UAV based upon active disturbance rejection control. *Aerosp. Sci. Technol.* **2018**, *79*, 601–609. [\[CrossRef\]](#)
22. Rsetam, K.A.; Cao, Z.; Man, Z. Cascaded Extended State Observer Based Sliding Mode Control for Underactuated Flexible Joint Robot. *IEEE Trans. Ind. Electron.* **2019**, *67*, 10822–10832. [\[CrossRef\]](#)
23. Zhang, Z.; Li, L.; Wu, Y. Disturbance-observer-based antishwing control of underactuated crane systems via terminal sliding mode. *IET Control Theory Appl.* **2018**, *12*, 2588–2594. [\[CrossRef\]](#)
24. De Plinval, H.; Morin, P.; Mouyon, P. Stabilization of a class of underactuated vehicles with uncertain position measurements and application to visual servoing. *Automatica* **2017**, *77*, 155–169. [\[CrossRef\]](#)
25. Belzile, B.; Birglen, L. Stiffness Analysis of Underactuated Fingers and Its Application to Proprioceptive Tactile Sensing. *IEEE/ASME Trans. Mechatron.* **2016**, *21*, 2672–2681. [\[CrossRef\]](#)
26. Hua, M.-D.; Hamel, T.; Morin, P.; Samson, C. A control approach for thrust-propelled underactuated vehicles and its application to VTOL drones. *IEEE Trans. Autom. Control* **2009**, *54*, 1837–1853.
27. Khan, Q.; Akmeliawati, R.; Bhatti, A.I.; Khan, M.A. Robust stabilization of underactuated nonlinear systems: A fast terminal sliding mode approach. *ISA Trans.* **2017**, *66*, 241–248. [\[CrossRef\]](#)
28. Shin, S.-Y.; Lee, J.-J. Fuzzy sliding mode control for an under-actuated system with mismatched uncertainties. *Artif. Life Robot.* **2010**, *15*, 355–358. [\[CrossRef\]](#)
29. Ravichandran, M.T.; Mahindrakar, A.D. Robust stabilization of a class of underactuated mechanical systems using time scaling and Lyapunov redesign. *IEEE Trans. Ind. Electron.* **2011**, *58*, 4299–4313. [\[CrossRef\]](#)
30. Sadeghian, H.; Ott, C.; Garofalo, G.; Cheng, G. Passivity-based control of underactuated biped robots within hybrid zero dynamics approach. In Proceedings of the IEEE International Conference on Robotics and Automation (ICRA), Singapore, 29 May–3 June 2017; pp. 4096–4101.
31. Colombo, L.; De Diego, D.M.; Zuccalli, M. Optimal control of underactuated mechanical systems: A geometric approach. *J. Math. Phys.* **2010**, *51*, 083519. [\[CrossRef\]](#)
32. Chhabra, R.; Emami, M.R. A unified approach to input-output linearization and concurrent control of underactuated open-chain multi-body systems with holonomic and nonholonomic constraints. *J. Dyn. Control Syst.* **2016**, *22*, 129–168. [\[CrossRef\]](#)
33. Azimi, M.M.; Kofigar, H.R. Adaptive fuzzy backstepping controller design for uncertain underactuated robotic systems. *Nonlinear Dyn.* **2015**, *79*, 1457–1468. [\[CrossRef\]](#)
34. Rudra, S.; Barai, R.K.; Maitra, M. Design of nonlinear state feedback control law for underactuated two-link planar robot: A block backstepping approach. In Proceedings of the Conference on Advances in Robotics, New York, NY, USA, 4–6 July 2013; pp. 1–6.
35. Sun, N.; Fang, Y.; Chen, H. A new antishwing control method for underactuated cranes with unmodeled uncertainties: Theoretical design and hardware experiments. *IEEE Trans. Ind. Electron.* **2015**, *62*, 453–465. [\[CrossRef\]](#)
36. Hasan, A.T. Under-actuated robot manipulator positioning control using artificial neural network inversion technique. *Adv. Artif. Intell.* **2012**, *2012*, 7. [\[CrossRef\]](#)
37. Moussaoui, S.; Boulkroune, A. Stable Adaptive Fuzzy Sliding-Mode Controller for a Class of Underactuated Dynamic Systems. In *Recent Advances in Electrical Engineering and Control Applications*; Springer: Cham, Switzerland, 2017; pp. 114–124.
38. Seifried, R. Two approaches for feedforward control and optimal design of underactuated multibody systems. *Multibody Syst. Dyn.* **2012**, *27*, 75–93. [\[CrossRef\]](#)
39. Rascón, R.; Alvarez, J.; Aguilar, L.T. Discontinuous  $H_\infty$  control of underactuated mechanical systems with friction and backlash. *Int. J. Control Autom. Syst.* **2016**, *14*, 1213–1222. [\[CrossRef\]](#)
40. Sun, N.; Fang, Y.; Zhang, X. An increased coupling-based control method for underactuated crane systems: Theoretical design and experimental implementation. *Nonlinear Dyn.* **2012**, *70*, 1135–1146. [\[CrossRef\]](#)
41. Schnelle, F.; Eberhard, P. Adaptive Model Predictive Control Design for Underactuated Multibody Systems with Uncertain Parameters. In *ROMANSY 21-Robot Design, Dynamics and Control*; Springer: New York, NY, USA, 2016; pp. 145–152.
42. Khan, Q.; Akmeliawati, R. Robust control of underactuated systems: Higher order integral sliding mode approach. *Math. Probl. Eng.* **2016**, *2016*. [\[CrossRef\]](#)
43. Din, S.; Khan, Q.; Rehman, F.; Akmeliawati, R. A Comparative Experimental Study of Robust Sliding Mode Control Strategies for Underactuated Systems. *IEEE Access* **2017**, *5*, 10068–10080. [\[CrossRef\]](#)
44. Alhato, M.M.; Ibrahim, M.N.; Rezk, H.; Bouallègue, S. An Enhanced DC-Link Voltage Response for Wind-Driven Doubly Fed Induction Generator Using Adaptive Fuzzy Extended State Observer and Sliding Mode Control. *Mathematics* **2021**, *9*, 963. [\[CrossRef\]](#)
45. Mouktonglang, T.; Worapun, P. A Comparison of Robust Criteria for Vehicle Routing Problem with Soft Time Windows. *Int. J. Math. Math. Sci.* **2019**, *2019*. [\[CrossRef\]](#)
46. Majumder, K.; Patre, B. Adaptive sliding mode control for asymptotic stabilization of underactuated mechanical systems via higher-order nonlinear disturbance observer. *J. Vib. Control* **2019**, *25*, 2340–2350. [\[CrossRef\]](#)
47. Xi, X.; Mobayen, S.; Ren, H.; Jafari, S. Robust finite-time synchronization of a class of chaotic systems via adaptive global sliding mode control. *J. Vib. Control* **2018**, *24*, 3842–3854. [\[CrossRef\]](#)



48. Truong, T.N.; Vo, A.T.; Kang, H.-J. A Backstepping Global Fast Terminal Sliding Mode Control for Trajectory Tracking Control of Industrial Robotic Manipulators. *IEEE Access* **2021**, *9*, 31921–31931. [\[CrossRef\]](#)
49. Khoo, S.; Xie, L.; Zhao, S.; Man, Z. Multi-surface sliding control for fast finite-time leader-follower consensus with high order SISO uncertain nonlinear agents. *Int. J. Robust Nonlinear Control* **2013**, *24*, 2388–2404. [\[CrossRef\]](#)
50. Mondal, S.; Mahanta, C. Chattering free adaptive multivariable sliding mode controller for systems with matched and mismatched uncertainty. *ISA Trans.* **2013**, *52*, 335–341. [\[CrossRef\]](#) [\[PubMed\]](#)
51. Bilgin, N.; Salamci, M.U. Sliding Mode Control Design For Nonlinear Systems without Reaching Phase and Its Applications to a Flexible Spacecraft. In Proceedings of the ASME 2014 12th Biennial Conference on Engineering Systems Design and Analysis, Copenhagen, Denmark, 25–27 June 2014; p. V002T007A005.
52. Mobayen, S. A novel global sliding mode control based on exponential reaching law for a class of underactuated systems with external disturbances. *J. Comput. Nonlinear Dyn.* **2016**, *11*, 021011. [\[CrossRef\]](#)
53. Liu, J.; Laghrouche, S.; Wack, M. Observer-based higher order sliding mode control of power factor in three-phase AC/DC converter for hybrid electric vehicle applications. *Int. J. Control* **2014**, *87*, 1117–1130. [\[CrossRef\]](#)
54. Sam, Y.M.; Osman, J.H.; Ghani, M.R.A. A class of proportional-integral sliding mode control with application to active suspension system. *Syst. Control Lett.* **2004**, *51*, 217–223. [\[CrossRef\]](#)
55. Plestan, F.; Shtessel, Y.; Bregeault, V.; Poznyak, A. Sliding mode control with gain adaptation—Application to an electropneumatic actuator. *Control Eng. Pract.* **2013**, *21*, 679–688. [\[CrossRef\]](#)
56. González, I.; Salazar, P.; Lozano, R. Chattering-free sliding mode altitude control for a quad-rotor aircraft: Real-time application. *J. Intell. Robot. Syst.* **2014**, *73*, 137–155. [\[CrossRef\]](#)
57. Baek, J.; Jin, M.; Han, S. A new adaptive sliding-mode control scheme for application to robot manipulators. *IEEE Trans. Ind. Electron.* **2016**, *63*, 3628–3637. [\[CrossRef\]](#)
58. Wang, Z. Adaptive smooth second-order sliding mode control method with application to missile guidance. *Trans. Inst. Meas. Control* **2017**, *39*, 848–860. [\[CrossRef\]](#)
59. Elmokadem, T.; Zribi, M.; Youcef-Toumi, K. Trajectory tracking sliding mode control of underactuated AUVs. *Nonlinear Dyn.* **2016**, *84*, 1079–1091. [\[CrossRef\]](#)
60. Nasir, M.T.; El-Ferik, S. Adaptive sliding-mode cluster space control of a non-holonomic multi-robot system with applications. *IET Control Theory Appl.* **2017**, *11*, 1264–1273. [\[CrossRef\]](#)
61. Huang, J.; Ri, S.; Fukuda, T.; Wang, Y. A disturbance observer based sliding mode control for a class of underactuated robotic system with mismatched uncertainties. *IEEE Trans. Autom. Control* **2018**, *64*, 2480–2487. [\[CrossRef\]](#)
62. Asl, R.M.; Hagh, Y.S.; Palm, R. Robust control by adaptive non-singular terminal sliding mode. *Eng. Appl. Artif. Intell.* **2017**, *59*, 205–217.
63. Patnaik, R.; Dash, P.; Mahapatra, K. Adaptive terminal sliding mode power control of DFIG based wind energy conversion system for stability enhancement. *Int. Trans. Electr. Energy Syst.* **2016**, *26*, 750–782. [\[CrossRef\]](#)
64. Xiong, J.; Gan, Q.; Ren, W. Boundedness of discretised non-linear systems under fast terminal sliding mode control. *IET Control Theory Appl.* **2016**, *10*, 2100–2109. [\[CrossRef\]](#)
65. Asl, S.B.F.; Moosapour, S.S. Adaptive backstepping fast terminal sliding mode controller design for ducted fan engine of thrust-vectoring aircraft. *Aerosp. Sci. Technol.* **2017**, *71*, 521–529.
66. Yu, X.; Zhihong, M. Fast terminal sliding-mode control design for nonlinear dynamical systems. *IEEE Trans. Circuits Syst. I Fundam. Theory Appl.* **2002**, *49*, 261–264.
67. Yu, S.; Guo, G.; Ma, Z.; Du, J. Global fast terminal sliding mode control for robotic manipulators. *Int. J. Model. Identif. Control* **2006**, *1*, 72–79. [\[CrossRef\]](#)
68. Li, S.-B.; Li, K.-Q.; Wang, J.-Q.; Yang, B. Nonsingular fast terminal-sliding-mode control method and its application on vehicular following system. *Control Theory Appl.* **2010**, *27*, 543–550.
69. Yang, L.; Yang, J. Nonsingular fast terminal sliding-mode control for nonlinear dynamical systems. *Int. J. Robust Nonlinear Control* **2011**, *21*, 1865–1879. [\[CrossRef\]](#)
70. Fei, J.; Yan, W. Adaptive control of MEMS gyroscope using global fast terminal sliding mode control and fuzzy-neural-network. *Nonlinear Dyn.* **2014**, *78*, 103–116. [\[CrossRef\]](#)
71. Li, H.; Dou, L.; Su, Z. Adaptive nonsingular fast terminal sliding mode control for electromechanical actuator. *Int. J. Syst. Sci.* **2013**, *44*, 401–415. [\[CrossRef\]](#)
72. Li, P.; Ma, J.; Zheng, Z.; Geng, L. Fast nonsingular integral terminal sliding mode control for nonlinear dynamical systems. In Proceedings of the IEEE 53rd Annual Conference on Decision and Control (CDC), Los Angeles, CA, USA, 15–17 December 2014; pp. 4739–4746.
73. Lee, S.H.; Park, J.B.; Choi, Y.H. Finite time control of nonlinear underactuated systems using terminal sliding surface. In Proceedings of the IEEE International Symposium on Industrial Electronics, Seoul, Korea, 5–8 July 2009; pp. 626–631.
74. Zhu, Q.; Yu, R.; Liu, Z. A discontinuous control law of an underactuated surface vessel based on fast terminal sliding mode. In Proceedings of the 8th World Congress on Intelligent Control and Automation (WCICA), Jinan, China, 6–9 July 2010; pp. 1168–1173.
75. Tian, Z.; Wu, H. Hierarchical terminal sliding mode control for underactuated space robots. In Proceedings of the International Conference on Machine Vision and Human-Machine Interface (MVHI), Kaifeng, China, 24–25 April 2010; pp. 195–198.



76. Wang, X.; Li, S. Finite-time trajectory tracking control of under-actuated autonomous surface vessels based on non-singular terminal sliding mode. *Aust. J. Electr. Electron. Eng.* **2012**, *9*, 235–246. [[CrossRef](#)]
77. Zheng, E.; Xiong, J. Quad-rotor unmanned helicopter control via novel robust terminal sliding mode controller and under-actuated system sliding mode controller. *Opt. Int. J. Light Electron Opt.* **2014**, *125*, 2817–2825. [[CrossRef](#)]
78. Khan, Q.; Bhatti, A.I.; Akmeiliawati, R. Robust stabilization of underactuated systems via fast terminal sliding mode. In Proceedings of the 10th Asian Control Conference (ASCC), Kota Kinabalu, Malaysia, 31 May–3 June 2015; pp. 1–6.
79. Liu, G.; Xu, G.; Chen, Y.; Zhang, W.; Wang, G.; Li, F. A Novel Terminal Sliding Mode Control for the Navigation of An Under-actuated UUV. In Proceedings of the 26th International Ocean and Polar Engineering Conference, Rhodes, Greece, 26 June–21 July 2016.
80. Yan, Z.-P.; Yu, H.-M.; Li, B.-Y. Bottom-following control for an underactuated unmanned undersea vehicle using integral-terminal sliding mode control. *J. Cent. South Univ.* **2015**, *22*, 4193–4204. [[CrossRef](#)]
81. Huang, X.; Yan, Y.; Zhou, Y.; Hao, D. Fast terminal sliding mode control of underactuated spacecraft formation reconfiguration. *J. Aerosp. Eng.* **2016**, *29*, 04016020. [[CrossRef](#)]
82. Hongbin, W.; Zelin, Y.; Zhen, Z. Rbf-based terminal sliding mode control for a class of underactuated mechanical system. In Proceedings of the Chinese Control and Decision Conference (CCDC), Yinchuan, China, 28–30 May 2016; pp. 664–667.
83. Yan, Z.-P.; Yu, H.-M.; Hou, S.-P. Diving control of underactuated unmanned undersea vehicle using integral-fast terminal sliding mode control. *J. Cent. South Univ.* **2016**, *23*, 1085–1094. [[CrossRef](#)]
84. Elmokadem, T.; Zribi, M.; Youcef-Toumi, K. Terminal sliding mode control for the trajectory tracking of underactuated Autonomous Underwater Vehicles. *Ocean. Eng.* **2017**, *129*, 613–625. [[CrossRef](#)]
85. Bhave, M.; Janardhanan, S.; Dewan, L. Configuration control of planar underactuated robotic manipulator using terminal sliding mode. *IFAC-PapersOnLine* **2016**, *49*, 148–153. [[CrossRef](#)]
86. Vaghei, Y.; Farshidianfar, A. Trajectory tracking of under-actuated nonlinear dynamic robots: Adaptive fuzzy hierarchical terminal sliding-mode control. *J. Artif. Intell. Data Min.* **2016**, *4*, 93–102.
87. Wang, Y.; Li, T.; Chen, C.P. Adaptive Terminal Sliding Mode Control for Formations of Underactuated Vessels. In Proceedings of the International Conference on Cognitive Systems and Signal Processing, Beijing, China, 19–23 November 2016; pp. 27–35.
88. Shikai, W.; Hongzhang, J.; Lingwei, M. Trajectory tracking for underactuated UUV using terminal sliding mode control. In Proceedings of the Chinese Control and Decision Conference (CCDC), Yinchuan, China, 28–30 May 2016; pp. 6833–6837.
89. Bayramoglu, H.; Komurcugil, H. Time-varying sliding-coefficient-based decoupled terminal sliding-mode control for a class of fourth-order systems. *ISA Trans.* **2014**, *53*, 1044–1053. [[CrossRef](#)] [[PubMed](#)]
90. Moulay, E.; Perruquetti, W. Finite time stability and stabilization of a class of continuous systems. *J. Math. Anal. Appl.* **2006**, *323*, 1430–1443. [[CrossRef](#)]
91. Chang, J.L. Dynamic output feedback integral sliding mode control design for uncertain systems. *Int. J. Robust Nonlinear Control* **2012**, *22*, 841–857. [[CrossRef](#)]
92. Wang, W.; Yi, J.; Zhao, D.; Liu, D. Design of a stable sliding-mode controller for a class of second-order underactuated systems. *IEE Proc. Control Theory Appl.* **2004**, *151*, 683–690. [[CrossRef](#)]